MOLECULAR AND CELLULAR BIOLOGY, July 2004, p. 6104–6115 Vol. 24, No. 13
0270-7306/04/$08.00+0 DOI: 10.1128/MCB.24.13.6104–6115.2004

Mice Deficient for All PIM Kinases Display Reduced Body Size and Impaired Responses to Hematopoietic Growth Factors†

Harald Mikkers,[1]‡ Martijn Nawijn,[1] John Allen,[1]§ Conny Brouwers,[2] Els Verhoeven,[1] Jos Jonkers,[2] and Anton Berns[1]*

Division of Molecular Genetics and Centre of Biomedical Genetics[1] and Division of Molecular Biology,[2] Netherlands Cancer Institute, 1066 CX Amsterdam, The Netherlands

Received 20 November 2003/Returned for modification 15 January 2004/Accepted 29 February 2004

The *Pim* family of proto-oncogenes encodes a distinct class of serine/threonine kinases consisting of PIM1, PIM2, and PIM3. Although the *Pim* genes are evolutionarily highly conserved, the contribution of PIM proteins to mammalian development is unclear. PIM1-deficient mice were previously described but showed only minor phenotypic aberrations. To assess the role of PIM proteins in mammalian physiology, compound *Pim* knockout mice were generated. Mice lacking expression of *Pim1*, *Pim2*, and *Pim3* are viable and fertile. However, PIM-deficient mice show a profound reduction in body size at birth and throughout postnatal life. In addition, the in vitro response of distinct hematopoietic cell populations to growth factors is severely impaired. In particular, PIM proteins are required for the efficient proliferation of peripheral T lymphocytes mediated by synergistic T-cell receptor and interleukin-2 signaling. These results indicate that members of the PIM family of proteins are important but dispensable factors for growth factor signaling.

The *Pim* family of proto-oncogenes consists of three members: *Pim1*, *Pim2*, and *Pim3*. They constitute a distinct class of protein kinases with specificity towards phosphorylation on serine/threonine residues (34), although the researchers conducting two studies have reported on additional tyrosine kinase activity displayed by human and *Xenopus* PIM, respectively (32, 39). *Pim1* was originally identified as a target for proviral activation in Moloney murine leukemia virus (M-MuLV)-induced T-cell lymphomas (7). In the mouse, *Pim1* encodes two proteins with short half-lives: a 33-kDa protein and a 44-kDa protein initiated from an upstream alternative (CUG) start codon (34). *Pim1* mRNA has a short half-life due to the presence of five copies of the AUUU(A) destabilization motif in the 3′ untranslated region (UTR) (34). *Pim2* and *Pim3* show strong homology to *Pim1* (2, 4, 12, 44). At the amino acid level PIM2 and PIM3 show 61 and 71% identity to PIM1, respectively. PIM2 shares many of the properties of PIM1: the mRNA and protein are labile, *Pim2* transcription can be initiated from upstream CUG codons (44), and Eμ*Myc* Eμ*Pim2* double transgenic mice develop B-lymphoid tumors comparable to those arising in Eμ*Myc* Eμ*Pim1* compound transgenic mice (3, 45). In addition, *Pim2* can effectively substitute for the *Pim1* oncogene in lymphomagenesis, as illustrated by the high number of activating proviral insertions near *Pim2* in MuLV-induced tumors in *Pim1*-deficient Eμ*Myc* transgenic mice (44). Since the 3′ UTR of *Pim3* also contains mRNA-destabilizing motifs and since *Pim3* can substitute for *Pim1* and *Pim2* in MuLV-induced lymphomagenesis, it is likely that PIM3 has activities that overlap with those of PIM1 and PIM2 (2, 25).

PIM proteins are widely expressed; together, they cover most if not all tissues. The highest *Pim1* mRNA levels are found in thymus and testis (35), whereas *Pim2* mRNA expression is the highest in brain and thymus (3) and *Pim3* mRNA is the most abundant in kidney (12). The three *Pim* members appear to be coexpressed during mouse development, although in some tissues a tendency towards expression of *Pim1* and *Pim3* or of *Pim2* and *Pim3* exists (11). The transcription of *Pim1* and *Pim2* is induced by a wide range of growth factors and mitogens: interleukin-2 (IL-2) (3, 8), IL-3 (3, 8), granulocyte-macrophage colony-stimulating factor (GM-CSF) and G-CSF (22), IL-4 (3), IL-5 (40), IL-6 (22), IL-7 (3, 9), IL-9 (3), IL-12, IL-15, alpha interferon (24), gamma interferon (3, 48), erythropoietin (26), thrombopoietin (TPO) (26), prolactin (6), concanavalin A (3), lipopolysaccharide (3), and phorbol myristate acetate (47). The majority of these factors transduce their primary signal through the JAK/STAT pathway, indicating that this cascade is probably instrumental in regulating the expression of the *Pim* genes. This notion is underscored by the presence of STAT-responsive elements in the *Pim1* promoter and was directly proven for the STAT3-mediated transactivation of *Pim1* induced by IL-6 (36).

The generation of *Pim1* mutant mice illustrated a role for PIM1 in growth factor signaling. Although no in vivo abnormalities were shown (20), PIM1-deficient pre-B cells and bone marrow-derived mast cells exhibit impaired in vitro proliferation in response to the presence of IL-7 and IL-3, respectively (9, 10). An important role for PIM1 in cytokine signaling was further implied by the PIM1-mediated rescue of a thymic cellularity defect in mice that lack the IL-2 receptor common-γ-chain. This rescue appears to be dependent on a functional CD3 complex, since a similar phenotype observed in CD3γ-

* Corresponding author. Mailing address: Division of Molecular Genetics and Centre of Biomedical Genetics, Netherlands Cancer Institute, Plesmanlaan 121, 1066 CX Amsterdam, The Netherlands. Phone: 31 20 5121990. Fax: 31 20 5122011. E-mail: a.berns@nki.nl.

† Supplemental material for this article may be found at http://mcb.asm.org.

‡ Present address: Cell and Molecular Biology Department, Karolinska Institutet, S-171 77, Stockholm, Sweden.

§ Present address: Cancer Drug Resistance Group, Centenary Institute of Cancer Medicine and Cell Biology, Newtown, NSW 2042, Australia.

deficient mice could not be rescued by the *Pim1* transgene (18). The absence of a significant phenotype in *Pim1*-deficient mice could be explained by a potential functional redundancy of PIM family members.

We generated compound *Pim1*$^{-/-}$ *Pim2*$^{-/-}$ *Pim3*$^{-/-}$ mice to address the role of the PIM family in mammalian development. While these mice are viable and fertile, their body size is reduced at birth and throughout postnatal life. Proliferation of hematopoietic cells in response to growth factors is impaired in vitro as well as in vivo in the absence of PIM. In addition, PIM proteins appear to be required for efficient cell cycle induction of peripheral T cells in response to synergistic T-cell receptor (TCR) and IL-2 signaling.

MATERIALS AND METHODS

Generation of compound-*Pim1*-, *Pim2*-, and *Pim3*-KO mice. The construction of the *Pim1 neo59* knockout (KO) line has been described previously (20, 41). *Pim2*- and *Pim3*-deficient animals were generated as follows: mouse genomic DNA fragments containing the complete *Pim2* or *Pim3* gene were isolated from a genomic λ-phage (λFIX) library derived from 129OLA inbred mice. For the *Pim2* targeting construct, genomic BamHI fragments encompassing *Pim2* exons 1, 2, and 3 were replaced with the hygromycin resistance gene (*Pgp*) controlled by the human *PGK* promoter. The *Pim3* KO construct was generated by replacing a genomic BstEII fragment, containing a part of exon 3, exons 4 to 5, and part of exon 6, with an internal ribosome entry site-β*Geo* (IRES-β*Geo*) cassette. The KO constructs were introduced into 129Ola-derived embryonic stem cells by electroporation and drug-resistant clones were selected using hygromycin and G418, respectively. Homologous recombinants were identified by Southern blot analysis using DNA probes located internally or externally with respect to the deleted region. Selected clones with normal karyotypes were injected into C57BL/6 blastocysts. Chimeric mice born from these embryos were crossed to FVB/N females to produce heterozygous mutant F_1 offspring. *Pim2*$^{+/-}$ F_1 mice were back-crossed to inbred *Pim1neo59* FVB/N mice for 10 generations, and F_{11} animals were intercrossed, yielding compound *Pim1*$^{-/-}$ *Pim2*$^{-/-}$ mice. *Pim3*$^{+/-}$ mice were bred to FVB/N mice for two generations and subsequently crossed to 11th-generation FVB/N *Pim1*$^{-/-}$ *Pim2*$^{-/-}$ mice. Progeny intercrosses yielded wild-type and all single KOs, as well as triple mutant animals. All mice were maintained under specific-pathogen-free conditions. All animal experiments were approved by the Dutch Animal Research Committee.

DNA and RNA analysis. *Pim2* and *Pim3* KO alleles were identified initially by Southern analysis of tail DNA restricted with EcoRI (*Pim2*) or SspI (*Pim3*); full-length mouse *Pim2* cDNA or a genomic DNA fragment 3′ to *Pim3* was used as a probe. Subsequently, *Pim* mutants were identified by PCR: the *Pim1* alleles were detected using *Pim1* and *Neo* primers (Pim1For, 5′-AAGCACGTGGAGAAGGACCG-3′; Pim1Rev, 5′-GACTGTGTCCTTGAGCAGCG-3′; NeoA, 5′-CGTCCTGCAGTTCATTCAGG-3′), the *Pim2* alleles with *Pim2* and *Pgp* primers (Pim2For, 5′-CACCGCGTCACGGATAGACG-3′; Pim2Rev, 5′-CCCACCTTCCACAGCAGCG-3′; HygroFor, 5′-AGCACTCGTCCGAGGGCAAAGG-3′; Pim2Rev2, 5′-CACGGTGGACCAGCCTAGC-3′), and the *Pim3* alleles with *Pim3* and *lacZ* primers (Pim3Sp1, 5′-CTGGACCAAATTGCTGCCCAC-3′; Pim3Sp4, 5′-GGATCTCTGGTTCAAGTATCC-3′; LacZ1, 5′-CGTCACACTACGTCTG-AACG-3′; LacZ2, 5′-CGACCAGATGATCACACTCG-3′).

For the tissue-specific expression of the different *Pim* members, total RNA was isolated using TriZol (Gibco BRL). Poly(A)$^+$ RNA was extracted from total RNA with PolyATract (Promega), separated by agarose gel electrophoresis, and blotted to Hybond-N membranes (Amersham). Northern blots were hybridized sequentially to full-length mouse *Pim1*, *Pim2*, and *Pim3* and human *GAPDH* cDNA probes. The full-length *Pim2* and *Pim3* cDNAs were cloned from a size-fractionated concanavalin A blast-derived cDNA λ-phage library.

We analyzed the expression of the *Pim1*, *Pim2*, and *Pim3* transcripts in splenocytes by reverse transcription-PCR (RT-PCR). For this, total spleen RNA was isolated using TriZol (Gibco BRL), treated with DNase, and reverse transcribed with random hexamer primers (Promega) and avian myeloblastosis virus-reverse transcriptase (Roche). The cDNA was amplified in a single PCR using Pim1For and Pim1Rev, Pim2For and Pim2Rev, or Pim3Sp1 and Pim3Sp4 primer combinations. As a control, *Gapdh* was amplified in the same PCR using Gapdh1 (5′-ACCGGATTTGGCCGTATT-3′) and Gapdh2 (5′-TCTGGGATGGAAATTGTGAG-3′).

Bone marrow colony assays. Mice (8 to 12 weeks of age) were sacrificed, and both femurs were flushed with Hank's balanced medium containing 50 mM HEPES (pH 7.4), 50 μM β-mercaptoethanol, and 20% fetal calf serum (FCS) (BioWhittaker). Nucleated bone marrow cells were counted in cell lysis buffer (StemCell Technologies). Cells were first diluted in Iscove's modified eagle medium (Gibco BRL) containing 50 μM β-mercaptoethanol and 2% FCS and were thereafter plated in duplicate in methylcellulose (M3234) (StemCell Technologies) containing the appropriate cytokines and growth factors. The cells were cultured at 37°C and 5% CO_2 under specific assay conditions as follows: for CFU-GM assays, $1.5 \cdot 10^4$ cells/ml, 10 ng of recombinant murine GM-CSF (Peprotech)/ml, 12 days; for CFU-Meg assays, $4 \cdot 10^5$ cells/ml, 40 ng of recombinant human TPO (R&D Systems)/ml, 8 days; for CFU-mix assays, $1.5 \cdot 10^4$ cells/ml, 10 ng of recombinant murine IL-3 (rmIL-3) (Peprotech)/ml, 12 days; for CFU-Eos assays, $2 \cdot 10^5$ cells/ml, 20 ng of rmIL-5 (R&D Systems)/ml, 15 days; for CFU-mix assays, $2 \cdot 10^5$ cells/ml, 50 ng of recombinant murine stem cell factor (SCF) (Peprotech)/ml, 12 days. After counting of the colonies, cultures were fixed in 4% formaldehyde and stained with a 2% Giemsa solution to determine the cell types.

T- and B-cell proliferation assays. Splenocytes and bone marrow cells were isolated from 8- to 12-week-old mice and counted in a Casy 1 counter (Schärfe Systems). Splenocytes were cultured in round-bottom 96-well plates at 10^6 cells per ml in complete medium (RPMI-1640 containing penicillin and streptomycin, glutamine, 50 μM β-mercaptoethanol, and 10% FCS) in the presence of recombinant human IL-2 (rhIL2) (R&D Systems) (concentrations as indicated in figures) and/or coated αCD3 (2C11) (Pharmingen) (concentrations as indicated in figures) for 48 h followed by 16 h with 0.5 μCi of [^{3}H]thymidine. Bone marrow cells were cultured in flat-bottom 96-well plates at 10^7 cells/ml in complete medium with 50 or 250 U of rmIL-7 (Peprotech)/ml for 3 days and for an additional 18 h in the presence of 0.5 μCi of [^{3}H]thymidine.

Flow cytometry. Thymocytes, splenocytes, and bone marrow cells from mice 6 to 8 weeks of age were isolated and analyzed by flow cytometry using fluorochrome or biotin-tagged antibodies (all Pharmingen) to CD3ε, Mac1, CD69, B220, BP1, CD62l, TCRβ, CD4, CD8, CD25 (IL2Rα), CD117, IL2Rβ, common-γ-chain, IL-7Rα, Sca1, heat-stable antigen (HSA), Gr-1, immunoglobulin M (IgM), IgD, and NK1.1. Biotinylated antibodies were detected using antigen-presenting-cell-conjugated streptavidin (Molecular Probes). Cells were stained in phosphate-buffered saline with 1% bovine serum albumin, 0.05% sodium azide, and 2% normal mouse serum.

Splenocytes were isolated from 8- to 12-week-old mice and cultured at a density of 10^6 cells/ml in the presence or absence of hIL-2 (200 U/ml) in 48-well plates coated with 0.3 μg of αCD3 (Pharmingen)/ml for the indicated time periods. Carboxyfluorescein diacetate succinimidyl ester (CFSE) (Molecular Probes) staining was performed according the manufacturer's protocol. Cells were labeled for 1 h after 24 h of culture with 10 μM bromodeoxyuridine (BrdU; La Roche). All cells were stained with αTCRβ or CD3 antibodies (Pharmingen) and, where appropriate, fixed in 0.25% paraformaldehyde and permeabilized in 0.1% Tween–phosphate-buffered saline. αBrdU-fluorescein isothiocyanate (La Roche) was used to detect BrdU incorporation, and cell-cycle profiles were analyzed using 7-aminoactinomycin D (7-AAD; Molecular Probes). Apoptotic cells were detected by terminal deoxynucleotidyltransferase-mediated dUTP-biotin nick end labeling staining according the manufacturer's protocol (La Roche) or with biotinylated annexin V (Molecular Probes), antigen-presenting-cell-conjugated streptavidin (Pharmingen), and propidium iodide (Molecular Probes). All cells were analyzed on a FACSCalibur flow cytometer (Becton Dickinson).

Western blot analysis. Splenocytes isolated from 8- to 12-week-old mice were cultured at 10^6 cells per ml in starvation medium (RPMI 1640 containing penicillin and streptomycin, glutamine, 50 μM β-mercaptoethanol, and 0.5% FCS) for 16 h. Cells were then treated with rhIL2 (R&D Systems) for 20 min (concentrations as indicated in legends to the figures), and whole cell lysates were prepared using standard 0.5% NP-40 lysis buffer. Lysates were separated using 10% polyacrylamide gel electrophoresis and blotted to nitrocellulose. STAT5 protein levels and STAT5 tyrosine phosphorylation were detected using antibodies from Transduction Labs-Becton Dickinson and Cell Signaling Technology (Beverly, Mass.), respectively.

RESULTS

Generation and initial characterization of *Pim* mutant mice. To inactivate *Pim2* and *Pim3* we designed targeting vectors that disrupted the kinase domains. The *Pim2* targeting vector contained the hygromycin resistance gene under the control of

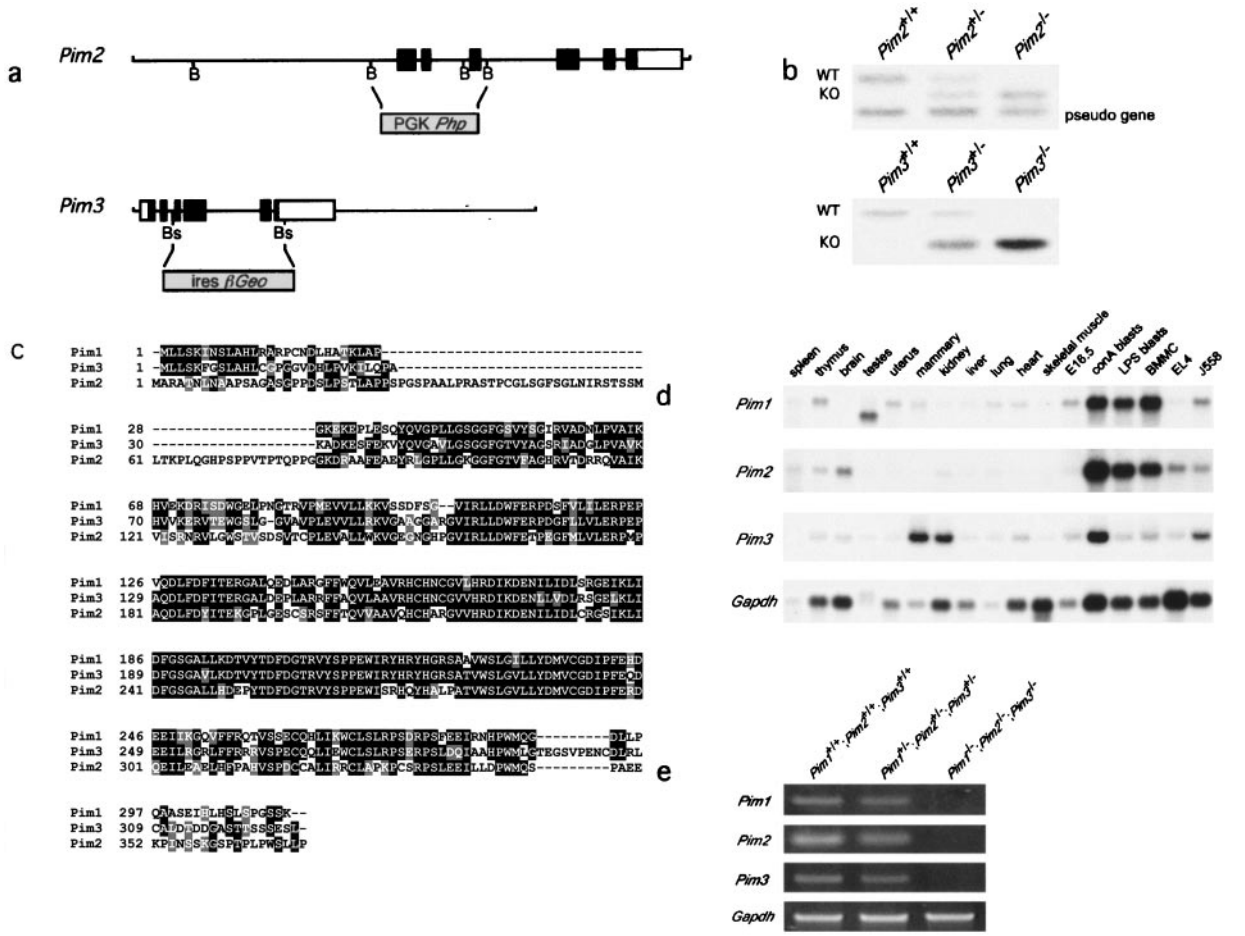

FIG. 1. The generation of *Pim1 Pim2 Pim3* compound KO mice. (a) Targeting constructs for *Pim2* and *Pim3*. PGK-*Php* was introduced into the BamHI (B) sites of *Pim2*, thereby deleting exons 1, 2, and 3. For *Pim3*, a part of exon 3, exons 4 and 5, and part of exon 6 were deleted through introduction of the promoterless IRES-β*Geo* cassette into the BstEII (Bs) sites. (b) Genotype analysis of *Pim2* and *Pim3* KO mice by Southern blotting using full-length *Pim2* cDNA or the 3′ UTR of *Pim3* as a probe. WT, wild type. (c) Comparison of the amino acid sequences of PIM1, PIM2, and PIM3. Identical residues are shown in white characters on a black background; similar residues are shown in white characters on a grey background. (d) Expression of *Pim1*, *Pim2*, and *Pim3* mRNA. The results are shown for bone marrow-derived mast cells grown on IL-3 (BMMC), EL4 (T-cell line), and J558 (plasmacytoma). LPS, lipopolysaccharide. (e) RT-PCR analysis of *Pim1*, *Pim2*, and *Pim3* expression in wild-type, Pim heterozygous, and Pim homozygous mutant splenocytes.

the human PGK promoter. Homologous recombination deletes exons 1, 2, and 3 (Fig. 1a). Since *Pim3* is expressed in embryonic stem cells, the *Pim3* targeting vector was constructed with the promoterless IRES-β*Geo* cassette (29), which replaces part of exon 3, exons 4 to 5, and part of exon 6 (Fig. 1a). Correctly targeted, karyotypically normal embryonic stem clones were injected into blastocysts to generate chimeric mice and, subsequently, homozygous *Pim2* or *Pim3* mutant mice (Fig. 1b). Both PIM2- and PIM3-deficient mice are viable, healthy, and fertile and do not show any gross abnormalities (data not shown).

The lack of an obvious phenotype in both the *Pim2* and *Pim3* mutants could be a consequence of redundancy with the remaining *Pim* genes, which is suggested by the amino acid homology and the overlap in expression of PIM1, PIM2, and PIM3 (Fig. 1c and 1d). Therefore, the *Pim2* and *Pim3* KO mice were crossbred with the previously described *Pim1* mutant mice, generating compound $Pim1^{-/-}$ $Pim2^{-/-}$ $Pim3^{-/-}$ mutants. Homozygous triple mutant mice were observed at a frequency expected for normal Mendelian segregation (data not shown). mRNA of the three *Pim* genes was undetectable by RT-PCR in the spleens of these mice, in contrast to the results seen with spleens from wild-type and $Pim1^{+/-}$ $Pim2^{+/-}$ $Pim3^{+/-}$ mice, confirming the functional deletion of the genes (Fig. 1e).

Mice deficient for *Pim1*, *Pim2*, and *Pim3* are smaller. *Pim* genes can act as potent oncogenes (3, 45). Whereas oncogene overexpression promotes cellular growth either by an increase in cell size or by an increase in cell number, the opposite may be expected when these genes are disrupted. Several oncogene KOs, including *Myc* and *CyclinD1*, do indeed display a size reduction of certain tissues (37, 43). The size of *Pim1* (20), *Pim2*, or *Pim3* single-KO mice is unaltered in comparison to that of wild-type mice. However, both mature male and mature female $Pim1^{-/-}$ $Pim2^{-/-}$ $Pim3^{-/-}$ mice are approximately 30% smaller than their $Pim1^{+/-}$ $Pim2^{-/-}$ $Pim3^{-/-}$, $Pim1^{-/-}$ $Pim2^{-/-}$ $Pim3^{+/-}$, $Pim1^{+/-}$ $Pim2^{-/-}$ $Pim3^{+/-}$, and wild-type littermates (Fig. 2a and b and data not shown). These size

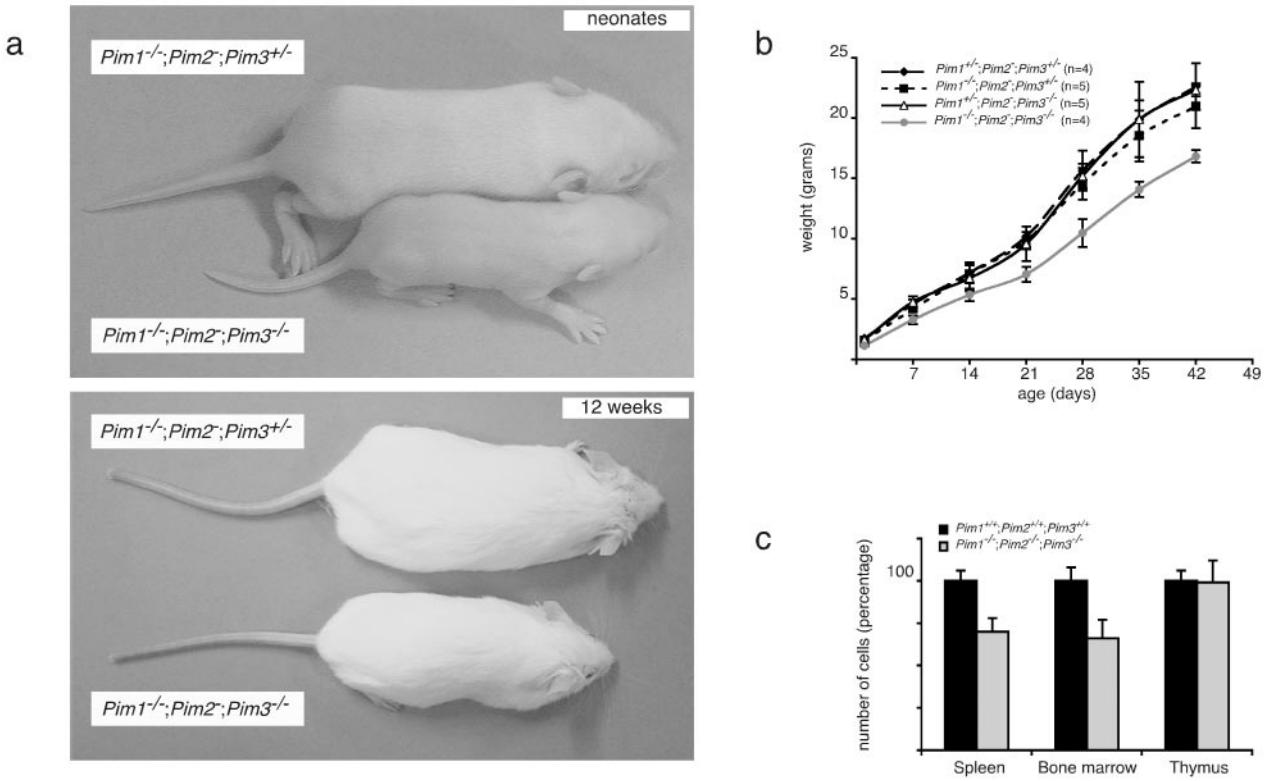

FIG. 2. PIM-deficient mice display a growth defect. (a) Comparison of male neonatal and mature *Pim1*$^{-/-}$ *Pim2*$^{-}$ *Pim3*$^{-/-}$ mice with *Pim1*$^{-/-}$ *Pim2*$^{-}$ *Pim3*$^{+/-}$ littermates (upper and lower panel, respectively). (b) Growth curve of male *Pim1*$^{+/-}$ *Pim2*$^{-}$ *Pim3*$^{+/-}$, *Pim1*$^{-/-}$ *Pim2*$^{-}$ *Pim3*$^{+/-}$, *Pim1*$^{+/-}$ *Pim2*$^{-}$ *Pim3*$^{-/-}$, and *Pim1*$^{-/-}$ *Pim2*$^{-}$ *Pim3*$^{-/-}$ littermates. The weight of *Pim1*$^{+/-}$ *Pim2*$^{-}$ *Pim3*$^{+/-}$ mice is similar to that of wild-type mice. (c) Cell numbers in spleens, bone marrows, and thymuses from 8-week-old wild-type ($n = 9$) and *Pim1*$^{-/-}$ *Pim2*$^{-/-}$ *Pim3*$^{-/-}$ ($n = 9$) mice.

differences are already apparent at birth, as *Pim1*$^{-/-}$ *Pim2*$^{-/-}$ *Pim3*$^{-/-}$ neonates weigh 1.15 (± 0.10) g ($n = 4$) whereas their *Pim1*$^{+/-}$ *Pim2*$^{-/-}$ *Pim3*$^{-/-}$, *Pim1*$^{-/-}$ *Pim2*$^{-/-}$ *Pim3*$^{+/-}$, and *Pim1*$^{+/-}$ *Pim2*$^{-/-}$ *Pim3*$^{+/-}$ littermates weigh 1.63 (± 0.05) ($n = 4$), 1.66 (± 0.22) ($n = 3$), and 1.70 (± 0.10) ($n = 6$) g, respectively. These results demonstrate a functional redundancy between the three *Pim* genes with respect to their effect on body size. Analysis of *Pim1*$^{-/-}$ *Pim2*$^{-/-}$, *Pim2*$^{-/-}$ *Pim3*$^{-/-}$, and *Pim1*$^{-/-}$ *Pim3*$^{-/-}$ compound KO mice revealed that loss of PIM1 and PIM3 contributes predominantly to body size reduction. Still, *Pim1*$^{-/-}$ *Pim2*$^{-/-}$ *Pim3*$^{-/-}$ mice are reduced in size compared to *Pim1*$^{-/-}$ *Pim3*$^{-/-}$ mice, indicating an additional PIM2 effect (data not shown).

Except for the thymus, all organs displayed a size reduction corresponding to the decrease in body weight. To address whether the decreased body weight can be attributed to a decrease in cell number or cell size or both, we analyzed the relative sizes and numbers of cells in spleen and bone marrow. Whereas the cell size was only slightly reduced in triple-KO (TKO) mice, the cell number in PIM-deficient bone marrow and spleen was decreased to the same extent as the body size, indicating that the reduction in body weight is mainly the result of a decrease in cell number (Fig. 2c).

Disruption of the *Pim* genes causes subtle changes in hematopoietic differentiation. The high levels of *Pim* expression in hematopoietic tissues and the oncogenic activity of PIM in hematopoietic tumors prompted us to investigate the effect of PIM inactivation on the development of the hematopoietic lineages. Whole-blood analysis did not show significant differences between PIM-deficient and wild-type mice in the number of granulocytes, monocytes, and thrombocytes (data not shown). *Pim* mutant mice displayed a slight increase in the number of red blood cells; however, the hematocrit was not altered, most likely because PIM-deficient erythrocytes have a decreased mean cell volume (data not shown). This phenotype is comparable to the erythrocyte phenotype previously described for *Pim1* KO mice (20), indicating that additional loss of *Pim2* and *Pim3* does not yield an additive effect.

Next, we examined the thymic differentiation of T lymphocytes. No differences between *Pim1 Pim2 Pim3* mutant and wild-type animals were observed in any of the subpopulations of differentiating T lymphocytes in the thymus (Fig. 3a). At the CD4/CD8 double-negative (DN) stage of T-cell differentiation, PIM-deficient mice displayed slightly higher levels of CD25 expression at DN2 and DN3 but no consistent differences were found in any of these fractions. Also, no differences between PIM-deficient and PIM-proficient animals were observed in the kinetics and levels of TCRβ expression in the transition from the CD4/CD8 DN to double-positive (DP) stage of development (data not shown). *Pim* mutant spleens have normal $CD4^+$ and $CD8^+$ T-cell numbers, displaying normal CD62L and CD44 profiles within the different populations (Fig. 3a and data not shown). Taken together, these data indicate that T-

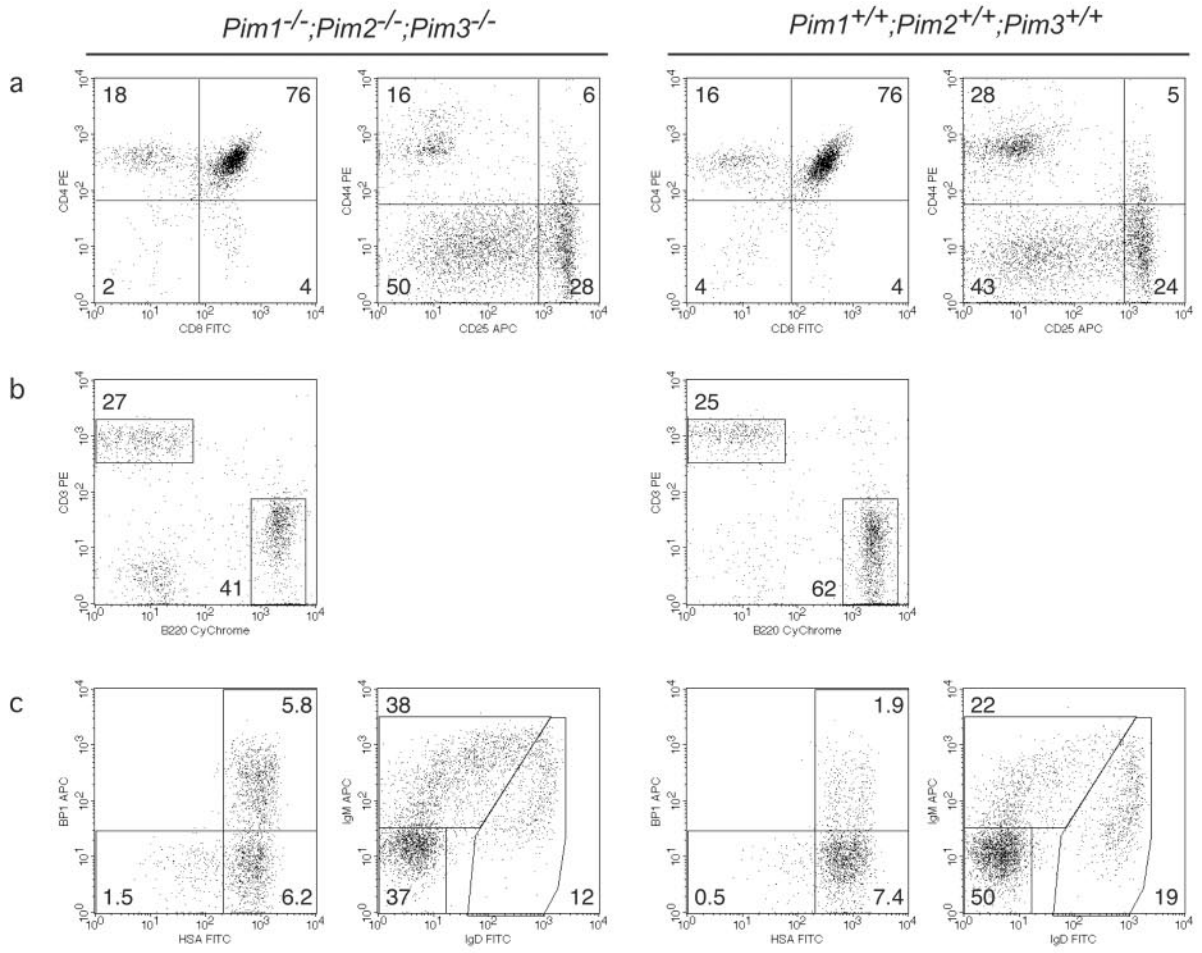

d

subpopulation	Pim1+/+/2+/+/3+/+	Pim1-/-/2-/-/3-/-
pre-pro B cells	0.53 ± 0.05	1.34 ± 0.06
pro B cells	7.2 ± 0.53	5.7 ± 0.22
pro & early pre-B cells	1.9 ± 0.13	5.4 ± 0.64
late pre B cells	53.9 ± 2.2	39.7 ± 1.0
IgM+ immature B cells	18.1 ± 2.1	22.8 ± 1.7
mature B cells	18.4 ± 0.6	14.1 ± 0.9

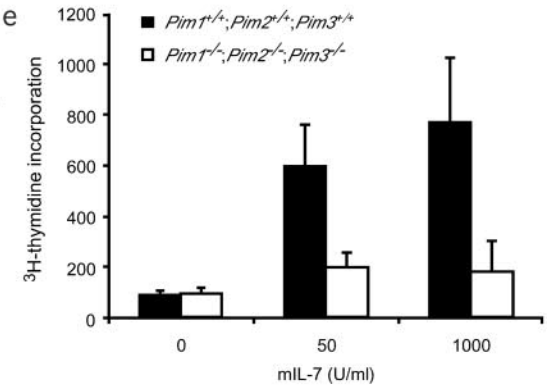

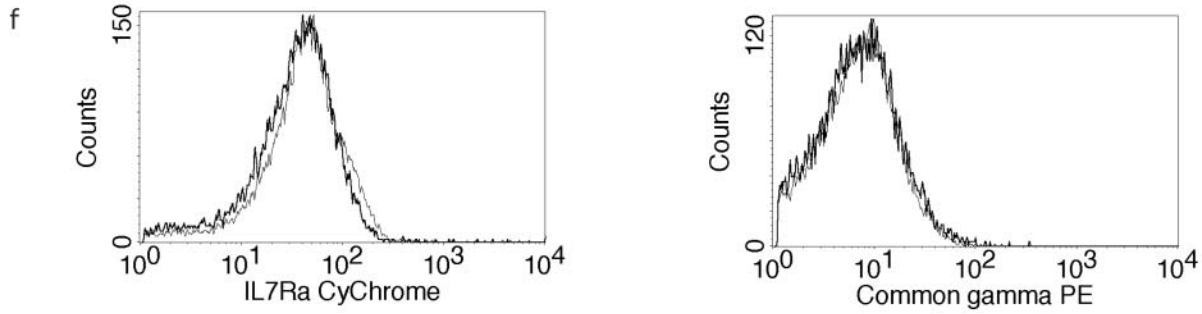

cell differentiation in and export from the thymus are unaffected by PIM deficiency.

In contrast to the T-cell results, the fraction of splenic B cells is reduced by approximately one-fourth in 8-week-old PIM-deficient mice compared to the results seen with age- and sex-matched wild types or *Pim* single mutants (Fig. 3b). The percentages of monocytes, granulocytes, and NK cells are comparable between *Pim* mutant and wild-type mice, whereas the erythroid progenitor fraction ($Ter119^+CD71^+CD117^+$) and the population of mature denucleated erythroid cells ($Ter119^+CD71^-$) are increased in *Pim* mutant spleens (data not shown). At 20 weeks of age, no differences between PIM-deficient and PIM-proficient animals were observed in B-cell numbers in spleen (data not shown).

In view of the reduction of the splenic B-cell fraction and the transforming activity of overexpressed PIM in immature B lymphocytes (3, 45), we analyzed B-cell differentiation in *Pim* mutant bone marrow (for a review, see reference 15). Plots from representative PIM-deficient (left panel) and wild-type (right panel) animals are shown in Fig. 3c; averages for this analysis are shown in Fig. 3d. Within the subpopulation of CD43-positive $B220^+$ B-cell progenitors, the early stages of B-cell development can be distinguished on the basis of the expression of HSA/CD24 and BP1. Pre-pro-B cells have not yet committed to the B-cell lineage and are characterized as HSA^{lo}/BP1-negative cells. PIM-deficient bone marrow contains an increased fraction of these cells (Fig. 3c and d). HSA^{hi}/BP1-negative cells are pro-B cells and seem to be present in slightly lower numbers in PIM-deficient bone marrow. Finally, HSA^{hi}/BP1-positive cells contain both noncycling cells, which are in the process of rearranging their heavy chains (pro-B cells), and proliferating cells (early pre-B cells), which have successfully rearranged their heavy-chain locus. Although the proliferation of the early pre-B cells is pre-B-cell-receptor (BCR) initiated, it is propagated by IL-7 (16). In *Pim* mutant mice, HSA^{hi}/BP1-positive cell levels are increased about threefold compared to wild-type control levels. After a certain number of cell divisions, differentiating B cells exit from the cell cycle, having lost expression of CD43, and initiate genomic rearrangements at the light-chain locus. These cells are characterized as CD43-negative, $B220^+$, surface Ig-negative cells (late pre-B cells). In *Pim* mutant bone marrow, the number of late pre-B cells is substantially decreased (Fig. 3c and d). The increase in pre-pro-B cells (HSA^{lo}/BP1 negative) and pro-B–early pre-B cells (HSA^{hi}/BP1 positive), as well as the decrease in late pre-B-cells, was consistent between all experiments (a total of ~20 animals of each genotype). Upon successful light-chain rearrangement, differentiating B cells, which now express a functional BCR complex at the cell surface, again enter a proliferative phase. PIM-deficient bone marrow contains an increased fraction of surface IgM-positive cells (Fig. 3c). However, the observed dissimilarity between wild-type and *Pim* mutant cells results differed between experiments. Finally, mature B cells, characterized by the expression of both IgD and IgM as well as by high levels of B220, recirculate into the bone marrow. In *Pim* mutant mice no reproducible differences were found for mature B cells. Additional analysis of the B-cell development in mice lacking only one *Pim* revealed that the major factor causing this defect is loss of PIM1 and that loss of PIM3 follows loss of PIM1 in importance, whereas PIM2 deficiency has almost no effect on B-cell development (data not shown).

These data indicate that *Pim* mutant bone marrow is relatively enriched for pre-pro-B cells and HSA^{hi}/BP1-positive cells (pro-B and early pre-B cells). Pre-pro-B cells have not yet committed to the B-cell lineage. HSA^{hi}/BP1-positive cells consist of cells in the process of rearranging their heavy-chain locus (pro-B cells) as well as cells that are actively cycling (early pre-B cells). The increase in these cells could, therefore, be caused by an impaired rearrangement at the heavy-chain locus (pro-B cells), by a prolonged proliferative expansion phase after successful rearrangement of the heavy-chain locus (early pre-B cells), or, in contrast, by less-efficient cell cycle progression in response to pre-BCR/IL-7 signaling causing a delay in the progression from early pre-B cells to late pre-B cells. Since the number of late pre-B cells, which are in the process of rearranging the light-chain locus, is decreased in PIM-deficient bone marrow, we hypothesized that the increase in the HSA^{hi}/BP1-positive fraction (pro-B/late pre-B cells) reflects an effect on the proliferation rather than the rearrangement of differentiating B cells.

IL-7-mediated proliferation of late pre-B cells is decreased in the absence of PIM. Since we used cell surface markers to delineate the functionally relevant subpopulation in bone marrow, we could not conclude whether an increase in the HSA^{hi}/BP1-positive cell levels can be attributed to an enhanced proliferation upon heavy-chain rearrangement (resulting in more cells staining for these surface markers) or an attenuated cell cycle progression in response to pre-BCR/IL-7-mediated activation (resulting in a delayed exit from early pre-B to late pre-B, leading to an increased fraction of cells staining for the surface profile).

To distinguish between these possibilities, we grew IL-7-driven pre-B-cell cultures in vitro. Proliferation assays of B-cell progenitors demonstrated that the in vitro proliferative re-

FIG. 3. B- but not T-lymphoid development is affected in *Pim* mutant mice. The first two columns represent PIM-deficient mice; the second series of two columns represents wild-type mice. FITC, fluorescein isothiocyanate; APC, antigen-presenting cells. (a) Flow cytometric analysis of wild-type and *Pim* mutant thymocytes by CD4/CD8 staining (panels 1 and 3) and CD25/CD44 staining on cells negative for CD4, CD8, B220, CD19, Mac1, Ter119, Gr-1, and NK1.1 (panels 2 and 4). (b) Mature B-cell and T-cell populations in *Pim* mutant and wild-type spleen. (c) Analysis of B-cell differentiation in the bone marrow. CD43-positive, B220-positive cells were gated and analyzed using BP1 and HSA markers to distinguish pre-pro-B, pro-B, and pro-B–early pre-B cells (panels 1 and 3). CD43-negative, B220-positive cells were gated and analyzed using IgM and IgD to distinguish late pre-B, IgM-positive immature B, and mature B cells (panels 2 and 4). (d) The number of cells belonging to distinct stages of B-cell development depicted as a percentage of total B220-positive cell numbers in the bone marrow of 6- to 8-week-old wild-type and *Pim* mutant mice. (e) Proliferation of *Pim* mutant bone marrow cells in response to IL-7. Bone marrow cells were cultured for 96 h in the presence of mIL-7. Proliferation was determined by $[^3H]$thymidine incorporation. For the last 16 h, cells were cultured in the presence of $[^3H]$thymidine. One representative of three independent experiments is shown. (f) Cell surface expression levels IL-7Rα and common-γ-chain on differentiating B cells in the bone marrow. The thin line represents wild-type cells; the thick line represents Pim-deficient cells.

TABLE 1. In vitro colony formation capacity of mutant PIM and wild-type bone marrow cells in response to distinct growth factors

Growth factor	Colony type	Mean (±SD) colony formation capacity (*n*) for mice of Genotype[a]				
		Pim1$^{+/+}$*2*$^{+/+}$*3*$^{+/+}$	*Pim1*$^{-/-}$*2*$^{+/+}$*3*$^{+/+}$	*Pim1*$^{+/+}$*2*$^{-/-}$*3*$^{+/+}$	*Pim1*$^{+/+}$*2*$^{+/+}$*3*$^{-/-}$	*Pim1*$^{-/-}$*2*$^{-/-}$*3*$^{-/-}$
IL-3	CFU-mix	382 ± 43 (16)	194 ± 53[b] (3)	381 ± 14 (2)	336 ± 55 (6)	120 ± 37[b] (12)
SCF	CFU-mix	119 ± 10 (16)	82 ± 20 (3)	126 ± 5 (2)	95 ± 21[b] (5)	64 ± 12[b] (12)
GM-CSF	CFU-GM	358 ± 32 (18)	402 ± 62 (2)	365 ± 30 (2)	385 ± 43 (3)	357 ± 42 (12)
TPO	CFU-Meg	17.9 ± 2.5 (9)	0.26 ± 0.31 (3)	19.6 ± 0.8 (2)	18 ± 3 (6)	0 ± 0[b] (9)
IL-5	CFU-Eos	19.6 ± 2.1 (10)	8 ± 5.7 (2)	20.4 ± 0.4 (2)	18.6 ± 6.3 (3)	2 ± 1[b] (9)

[a] Values represent numbers of colonies. *n*, number of mice. *Pim1*$^{+/+}$*2*$^{+/+}$*3*$^{+/+}$, *Pim1*$^{+/+}$ *Pim2*$^{+/+}$ *Pim3*$^{+/+}$.
[b] $P < 0.05$ (*t* test analysis compared to the wild type).

sponse to IL-7 is severely impaired in *Pim* mutant bone marrow cells (Fig. 3e), arguing against an increased proliferative response to IL-7 in vivo. To ensure that the diminished response to IL-7 was not the result of decreased expression of the IL-7 receptor complex, we analyzed the expression of the IL-7Rα and common-γ-chain on differentiating B cells in the bone marrow. IL-7Rα expression of immature B cells in Pim-deficient mice is marginally decreased compared to wild-type mouse results (Fig. 2f), whereas common-γ-chain expression levels were essentially the same (Fig. 2f). These data indicate that the differentiating *Pim*-deficient B cells might be slightly less sensitive to IL-7-induced signaling, but it seems unlikely that this difference in receptor expression is responsible for the observed differences in the IL-7-induced proliferative response.

In analyzing the contributions of the individual PIM family members to this phenotype, it can be shown that the extent of the observed in vivo defect (increased presence of the HSA^{hi}/BP1-positive cells) correlated inversely with the ability to proliferate in response to the presence of IL-7 in vitro (see Fig. SA in the supplementary material). Although *Pim1* and *Pim3* are in part redundant, *Pim1* is the most critical family member for modulating IL-7-driven proliferation of these immature B cells (see Fig. SA in the supplementary material). Taken together, these data suggest that the increased subpopulation of CD43^{+}/B220^{+} cells that are HSA^{hi}/BP1 positive in PIM-deficient bone marrow can be attributed, at least partially, to a decreased proliferative response to IL-7.

PIM affects cytokine-mediated cell growth and differentiation of bone marrow cells. The induction of *Pim* expression is an early response to a variety of growth factors involved in hematopoiesis and is likely mediated by JAK/STAT signaling, as has been shown for IL-6-induced *Pim1* expression (36). JAK-deficient as well as STAT-deficient hematopoietic progenitors show a reduction in their capacity to form colonies in response to distinctive growth factors (for a review, see reference 17). The growth of *Pim1* mutant bone marrow-derived mast cells in response to the presence of IL-3 was previously shown to be diminished (10). Hence, to characterize the contribution of PIM proteins to myeloid and erythroid differentiation in response to growth factors, we performed colony formation assays of distinct *Pim* mutant hematopoietic progenitor populations (Table 1).

IL-3 signaling induces *Pim1* and *Pim2* very efficiently and *Pim3* to a lesser extent (Fig. 1d). The response of PIM-deficient bone marrow cells to the presence of IL-3 was strongly impaired, as indicated by a reduction in both colony number (approximately threefold) and colony size. Giemsa staining revealed that mixed hematopoietic colonies derived from PIM-deficient marrow contained cells predominantly of the erythroid lineage (see Fig. SB in the supplementary material), suggesting a substantial block in IL-3-dependent myeloid development. Although loss of PIM1 substantiates the largest effect, the additional loss of PIM2 and PIM3 does enhance the observed defect ($P = 0.026$). The disruption of all *Pim* genes decreases the granulocyte/macrophage content of IL-3-dependent CFU-mix colonies. However, the ability of *Pim* mutant bone marrow progenitors to form colonies in response to the presence of GM-CSF was unimpaired (Table 1) in spite of the fact that the GM-CSF receptor is a close family member of the IL-3 receptor and potently induces *Pim* expression (22). TPO stimulates the development of megakaryocytes. *Pim* mutant bone marrow cells were unable to differentiate into megakaryocytes in vitro, and again the loss of *Pim1* displayed the largest effect. In in vivo experiments, we observed fewer and hypoproliferative megakaryocytes in spleen sections, as evidenced by the absence of mitotic cells (data not shown). Moreover, formation of eosinophilic granulocytes in vitro in response to IL-5 was impaired; it seems as if this had also been predominantly mediated by PIM1 loss, although once again the additional loss of PIM2 and PIM3 considerably enhanced the effect. Lastly, a reduction in the number (50% of wild-type numbers) and size of colonies was also seen in the response of *Pim1 Pim2 Pim3* mutant bone marrow cells to the presence of SCF, a growth factor that signals via the KIT tyrosine kinase receptor and poorly induces *Pim* expression (3, 10). In contrast to IL-3-mediated colony formation, SCF showed an effect on growth and size of the colonies but not on the outgrowth of the different lineages within the colonies (data not shown).

PIM affects T-cell proliferation in response to TCR and IL-2 signaling. Since we observed no effect of PIM deficiency on T-lymphocyte differentiation in vivo, we assumed that peripheral T cells have been selected in a similar manner for the functionality of the TCR complex in both PIM-proficient and PIM-deficient mice. Therefore, we used peripheral T lymphocytes to study activation-induced proliferative responses of lymphocytes in the absence of PIM. IL-2 signaling efficiently induces *Pim* transcription (3, 8), and IL-2 signal transduction, like that of IL-7, is in part mediated by the common-γ-chain receptor. IL-2-induced signals display a strong synergy with TCR-mediated T-cell activation, which has also been shown to induce *Pim1* expression (47). Therefore, we first analyzed the proliferation of *Pim* mutant peripheral T cells in response to CD3 cross-linking. *Pim* mutant T cells stimulated by CD3

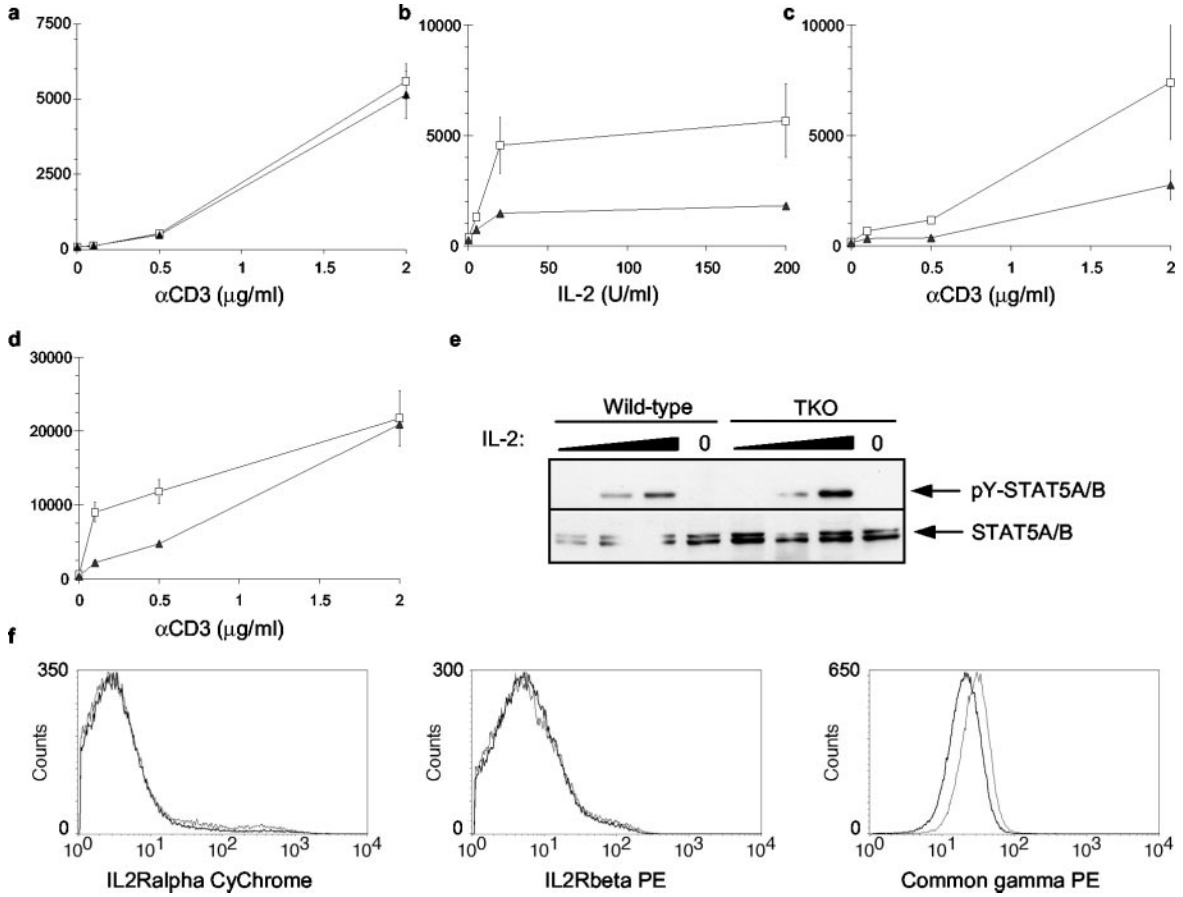

FIG. 4. The loss of PIM proteins affects [^{3}H]thymidine incorporation induced by synergistic TCR and IL-2 signaling. Splenic T lymphocytes derived from wild-type mice (open squares) or PIM-deficient mice (closed triangles) were cultured for 64 h in the presence of different concentrations of coated αCD3 (a), a suboptimal concentration of coated αCD3 (0.3 μg/ml) and increasing concentrations of hIL-2 (b), constant hIL-2 (5 U/ml) and increasing amounts of coated αCD3 (c), or constant hIL-2 (200 U/ml) and increasing amounts of αCD3 (d). The proliferation of T lymphocytes was assayed by measuring [^{3}H]thymidine incorporation for the last 16 h of culture. Each panel represents one of three independent experiments with similar results ($n = 3$ for each genotype). (e) STAT5 phosphorylation in response to a dilution series of 0.02, 2.0, and 200 U of IL-2 of wild-type and PIM-deficient spleen cells. (f) Cell surface expression of components of the IL-2R complex on splenic T cells of wild-type mice (open squares) and TKO mice (solid triangles). PE, phycoerythrin.

cross-linking alone incorporated [^{3}H]thymidine at rates similar to those seen with wild-type T cells (Fig. 4a). When T cells were activated by suboptimal levels of αCD3 and a dilution series of IL-2, however, PIM-deficient T cells exhibit a reduced proliferation, as indicated by a two- to fourfold reduction in [^{3}H]thymidine incorporation (Fig. 4b). A significant reduction was also observed for *Pim2* mutant T cells but not for cells from *Pim1* or *Pim3* single KOs (see Fig. SC in the supplementary material).

To address whether the difference in proliferation is dependent on TCR activation, T cells were activated with different doses αCD3 in the presence of low (5 U/ml) or high (200 U/ml) levels of IL-2 (Fig. 4c and 4d). PIM-deficient T cells displayed a reduced proliferation at suboptimal levels of αCD3 irrespective of the IL-2 concentration, which confirms the data in Fig. 2b. However, this difference disappeared at high levels of αCD3 (2 μg/ml) in the presence of high levels of IL-2 (200 U/ml; Fig. 4d). These results indicate that PIM-deficient T cells display normal proliferative responses at optimal levels of αCD3 and hIL2 but that PIM proteins are required for proper proliferation upon suboptimal stimulation of either signaling pathway in vitro.

To determine whether expression levels of IL-2R complex components could be contributing to the observed decreased responses, we analyzed the expression levels of IL-2Rα, IL-2Rβ, and common-γ-chain on mature peripheral T cells (Fig. 4f). The expression levels of IL-2Rα and IL-2Rβ between wild-type and TKO mice were similar. However, Pim-deficient peripheral T cells expressed decreased levels of common-γ-chain on their cell surfaces. To elucidate whether the difference in common γ-chain expression also resulted in less-efficient STAT5 phosphorylation upon IL-2-induced signaling, we analyzed STAT5 phosphorylation in response to a dilution series of IL-2. We did not observe a difference between wild-type and TKO T cells in STAT5 phosphorylation upon IL-2 treatment (Fig. 4e). This indicates that the proliferative defect observed in PIM-deficient T cells is not caused by decreased STAT5 phosphorylation in response to the presence of IL-2.

PIM is required for efficient cycling of peripheral T cells. The PIM proteins have been suggested to play an important

role in proliferation (5, 28, 30, 31, 36); however, several of these reports and others have provided additional evidence for an antiapoptotic function of PIM (13, 28, 30, 31, 33, 36, 46). Since an apparent decrease in the incorporation of [^{3}H]thymidine can be caused by decreased proliferation or decreased survival or a combination of the two, we investigated these processes in PIM-deficient peripheral T cells.

The apoptotic index and cell viability of peripheral T cells cultured in the presence of suboptimal levels of αCD3 and 200 U of hIL2 for 24 and 48 h were determined using Annexin V, 7-AAD, and terminal deoxynucleotidyltransferase-mediated dUTP-biotin nick end labeling staining. These analyses showed that the rate of apoptosis in PIM-deficient T-cells is not affected (Fig. 5a and data not shown).

Since the defect in [^{3}H]thymidine incorporation was predominantly apparent in *Pim2* single mutant and *Pim* compound KO T cells, we labeled wild-type and KO cells of both types with CFSE to track the number of cell divisions. After 48 h of culture in the presence of αCD3 and IL-2, 45% of the *Pim* mutant T cells had not yet divided compared to only 17% of the wild-type T cells. In addition, the proportion of PIM-deficient T cells that had divided more than once (14%) was markedly decreased compared to that of wild-type T cells (39%) (Fig. 5b). After 72 h, most of the PIM-deficient T-cells had divided at least once but they still lagged behind compared to their wild-type counterparts (Fig. 5c). Similar results were obtained by BrdU pulse labeling of the cells after 24 h of culturing under the same conditions (Fig. 5d). Also, for *Pim2* mutant T cells the [^{3}H]thymidine data correlated to a decrease in the number of cell divisions (see Fig. SC in the supplementary material).

Taken together, these data indicate that PIM-deficient T cells display a reduced proliferative response to suboptimal αCD3 activation in the presence of IL-2 due to a reduced capacity to undergo cell division under these conditions. No contribution of an enhanced induction of apoptosis was observed. Since the difference in the fractions of cells which had divided more than once did not increase in PIM-proficient T-cell cultures between 48 and 72 h compared to PIM-deficient T-cell culture results and since cells which had undergone multiple rounds of cell division were readily detected in PIM-deficient T-cell cultures, it seems that the observed diminished efficiency of cell cycle progression was specific for the first cell division of resting T cells.

DISCUSSION

In this study we analyzed the effect of targeted disruption of all PIM family members on murine development and hematopoietic differentiation. Surprisingly, the combined deficiency for all PIM family members resulted in a rather mild phenotype for the resultant compound *Pim* mutant mice. In light of the strong conservation of *Pim* genes between different species, this mild phenotype argues against a role for PIM family members in critical developmental processes. Apparently, life is compatible with the absence of PIM. On the other hand, the absence of an obvious phenotype in vivo under homeostatic conditions might in part be explained by the nature of *Pim* genes as early-response genes responding to growth factors and cytokines. In fact, critical functions of PIM family members might only be revealed under conditions of high stress, which severely disrupt the homeostatic situation.

We demonstrated that PIM proteins are important for body growth, since *Pim1 Pim2 Pim3* compound KO mice display a profound reduction in body size at birth and throughout their entire live span. The decrease in body size was predominantly caused by a reduction in the number of cells rather than cell size, although a minor cell-size difference was consistently observed between PIM-proficient and -deficient animals. The reduction in body size (approximately 30%) observed at birth is, as such, reminiscent of a defect in insulin-like growth factor (IGF)-insulin signaling. Mice carrying defects in either of these pathways display a reduction in body size ranging from 20 to 60%, depending on the nature of the defect (for a review, see reference 1). However, it remains to be determined whether IGF-insulin signaling is indeed affected in *Pim* mutant mice.

The majority of hematopoietic growth factors are efficient inducers of *Pim1*, *Pim2*, and *Pim3*. In addition, a role for PIM1 in the proliferative response of hematopoietic cells to the presence of IL-3 and IL-7 was demonstrated in experiments with *Pim1* KO bone marrow cells (9, 10). The generation of *Pim1*$^{-/-}$ *Pim2*$^{-/-}$ *Pim3*$^{-/-}$ compound KO mice and the subsequent isolation of PIM-deficient bone marrow cells demonstrated that PIM1, PIM2, and PIM3 can act redundantly in stimulating the colony formation of bone marrow cells in response to the presence of IL-3, IL-5, SCF, and TPO. It should, however, be noted that it seems that PIM1 is the most and PIM2 is the least crucial PIM protein in these responses. Since PIM2 is more efficiently induced than PIM3 by a number of these growth factors, PIM2 might have a role distinct from the functions of PIM1 and PIM3 in these settings. In contrast to results seen with respect to the response to IL-3, IL-5, SCF, and TPO, we did not observe an effect of PIM deficiency on the GM-CSF response. This is very remarkable, in particular because the receptor for GM-CSF is highly related to the IL-3 and IL-5 receptors, as they share the same common-β-chain, which acts as the signaling module. Thus, although GM-CSF signaling leads to transcriptional activation of *Pim* (22), the PIM proteins appear not to be necessary for efficient transduction of the GM-CSF signals. This is in contrast to the very similar IL-3 and IL-5 signaling, in which PIM kinases seem to play an important role.

In addition to the impaired colony formation of PIM-deficient bone marrow cells in response to a variety of growth factors, PIM-deficient early pre-B cells showed a reduced proliferative response to IL-7 in vitro. This was reflected in vivo by an attenuated progression of pro-B cells through the IL-7-driven proliferative stage that follows successful rearrangement of the heavy chain. Since differentiating B cells in the bone marrow of Pim-deficient animals show only marginally decreased IL-7Rα expression levels, it seems unlikely that the attenuated proliferative response to IL-7 can be attributed to lower IL-7R expression levels. In young animals, peripheral B-cell numbers were reduced, whereas in older animals, this was not the case. The observation that the number of B cells is unaltered in the periphery of older animals is likely explained by the continuous supplying of newly formed B cells from the bone marrow into the peripheral B-cell compartment and homeostatic proliferation of peripheral B cells (for a review, see reference 42).

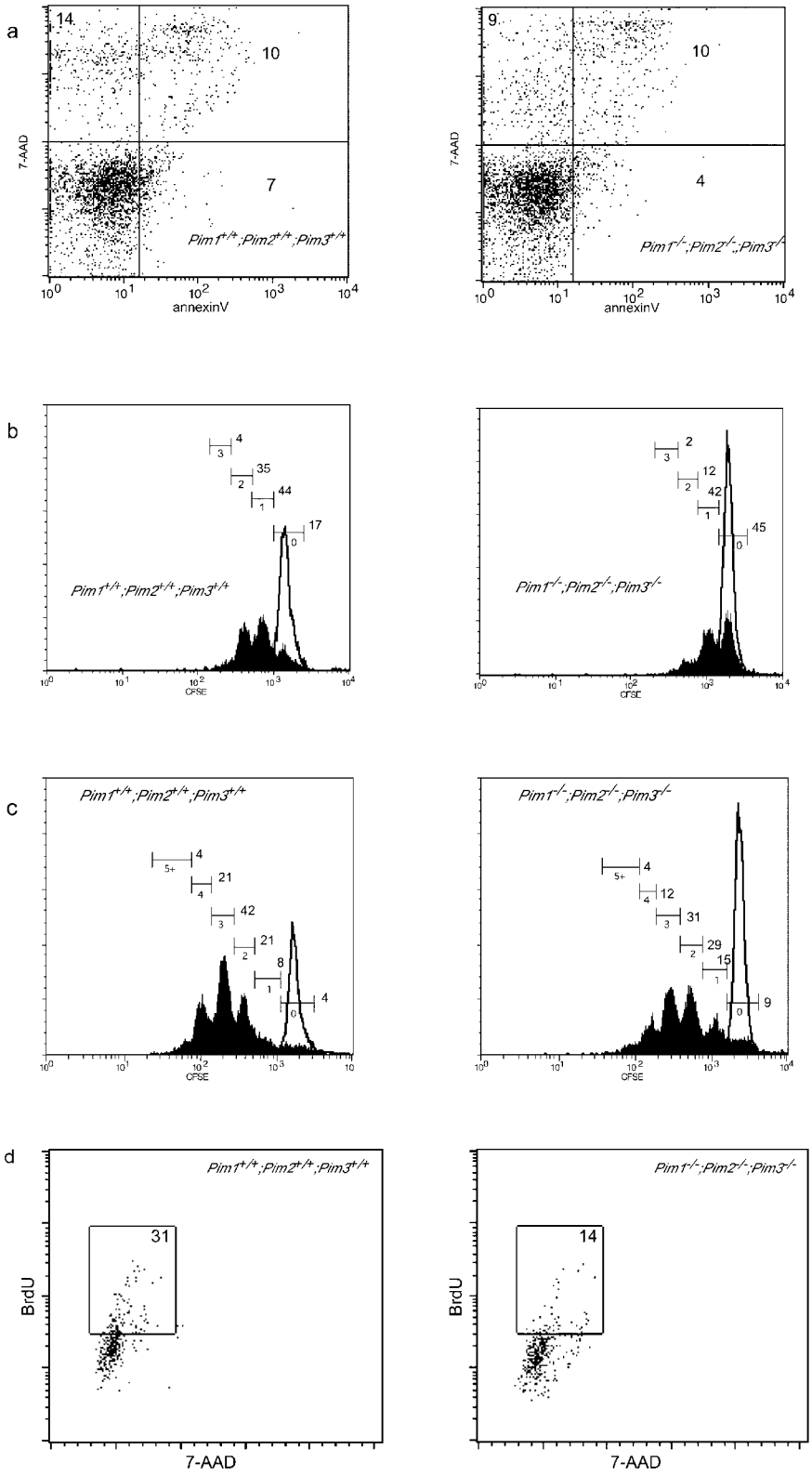

FIG. 5. PIM proteins appear to facilitate cell cycle entry in response to TCR and IL-2 signaling. Splenic T lymphocytes derived from wild-type or PIM-deficient mice were cultured in the presence of αCD3 (0.3 μg/ml) and hIL-2 (200 U/ml). For all analyses the T-cell population was characterized by flow cytometry using αTCRβ or αCD3 antibodies. (a) The proportions of apoptotic and dead cells after 48 h of culturing, as determined by Annexin V and 7-AAD staining. (b to c) The number of cell divisions was determined after 48 h (b) or 72 h (c) of culture growth, with CFSE used as a tracking dye (black lines correspond to unstimulated cells). (d) Analysis of DNA synthesis after 24 h of culture growth in the presence of hIL-2 (200 U/ml) and αCD3 (0.3 μg/ml).

The differentiation of T cells in the thymus is also characterized by a series of alternating phases of genomic recombination (resting cells) and IL-7-driven proliferation. We did not observe any effect of the absence of PIM on T-cell differentiation in the thymus. Although *Pim* mutant mice do not display abnormalities in thymic T-cell differentiation, the ability of peripheral T cells to proliferate in response to synergistic IL-2 and TCR activation was markedly impaired. The proliferative response of *Pim*-deficient and *Pim*-proficient T cells to a dilution series of CD3-cross-linking antibodies was identical. Likewise, serial dilutions of IL-2 on peripheral T cells elicited the same responses in terms of proliferation and STAT5 phosphorylation in both *Pim*-deficient and -proficient T cells. Yet when the two stimuli are combined, *Pim*-deficient T cells display a decreased response to the combined activities when either stimulus is present at suboptimal levels. PIM mutant peripheral T cells express lower levels of common-γ-chain but normal levels of the IL-2Rα and IL-2Rβ chains. This might indicate that common-γ-chain-transduced signals contribute to the decreased proliferation of PIM-deficient T cells. However, we did not find differences in STAT5 phosphorylation between PIM-proficient and PIM-deficient T cells. Moreover, it has been shown that the common-γ-chain is not required for antigen-driven proliferation of naïve T cells (21), indicating that additional mechanisms are likely to contribute to the decreased proliferation of peripheral T cells in response to the IL-2 and TCR activation. Further analysis of this proliferation defect demonstrates that PIM appears to be important for cell cycle entry of resting peripheral T cells at suboptimal levels of TCR signaling. PIM2 appeared to be the most critical PIM protein for this response, although PIM1 and PIM3 also contribute. These results indicate that the PIM proteins can augment the response to growth factor signals either directly or indirectly. The indirect pathway could involve signaling via the IGF receptors, as both IGF-I and -II can potentiate proliferation in B and T cells (14, 19). Such a role for PIM would also be consistent with previous results showing that overexpression of PIM1 can rescue the reduced thymic cellularity in common-γ-chain-deficient mice but only in the context of a functional CD3 complex (18).

We found no evidence that PIM deficiency compromises the survival of peripheral T cells. The results of other studies indicated that in vitro overexpression of PIM proteins protects cells against apoptosis (13, 28, 30, 31, 33, 36, 46). This apparent discrepancy emphasizes the notion that gene inactivation and overexpression studies do not necessarily reveal the same physiologically relevant functions of a protein. On the one hand, ectopic overexpression of proteins might evoke effects that are not representative of its function under physiological conditions. On the other hand, inactivation might elicit compensation by other proteins, obscuring or mitigating the normal role of the protein of interest. With respect to PIM proteins, which are usually expressed during a short time period due to the short half-lives of both mRNA and protein, overexpression studies using cells with enhanced PIM activity for prolonged periods are likely to yield data different from data obtained with studies using cells from which PIM activity had been deleted. The former situation might be more reflective of the role of PIM proteins during cellular transformation as observed in M-MuLV-induced tumors, whereas the latter could give more insight into the physiological role of PIM proteins in nontransformed cells. Therefore, the observation that an absence of PIM proteins does not give rise to cells which are more susceptible to apoptosis is not in contradiction with the notion that overexpression of PIM proteins might provide protection from apoptosis. The results from our study appear to be in agreement with *Pim1*- and *Pim2*-deficient mouse results from retroviral insertional mutagenesis screenings designed to identify genes that can substitute for PIM function in lymphomagenesis (25). The genes identified in this screen (e.g., *Kit* and *Ccnd2*) all regulate the G_1 to S transition. Therefore, although we cannot exclude the possibility that rescue from apoptosis is indeed a function of PIM proteins in lymphomagenesis, it seems that regulation of cell cycle is at least as important.

Since *Pim* expression is directly regulated by the JAK/STAT pathway (36), the *Pim* mutant phenotypes described here might provide clues about the biological significance of the STAT proteins for transactivation of the *Pim* genes. In fact, *Stat5a Stat5b* compound KO bone marrow cells display a reduced ability to form colonies in response to the presence of IL-3, IL-5, IL-7, SCF, GM-CSF, and TPO (37). Thus, the inability of STAT-deficient cells to induce *Pim* expression might be responsible for some of the observed signaling defects. In particular, STAT-deficient T cells cannot proliferate in response to TCR/IL-2 signaling (27). Although this phenotype is much stronger than the defect observed in *Pim* mutant T cells, our data show that the induction of PIM proteins has a significant effect on TCR/IL-2-mediated proliferation.

In summary, the phenotypes of the *Pim1 Pim2 Pim3* compound-KO mice illustrate a role for the PIM proteins in single-growth-factor signaling and in synergistic signaling pathways. The results with respect to synergistic growth factor signaling would suggest a view that PIM proteins might act as sensitizers of these pathways. This view would fit the induction of early transcription of the *Pim* genes by growth factors and the instability of the PIM mRNAs and proteins. Although such interplay between growth factor signals has been postulated before, the mediators have remained obscure. We show here that PIM proteins might fulfill such a role.

ACKNOWLEDGMENTS

We thank P. Krimpenfort and K. van Veen for blastocyst injections, L. Tolkamp and H. Starreveld for animal care, and L. Oomen for confocal microscopy assistance.

This work was supported by the Dutch Cancer Society (H.M. and M.N.) and the Leukemia and Lymphoma Society of America (J.A.).

REFERENCES

1. **Accili, D., J. Nakae, J. J. Kim, B. C. Park, and K. I. Rother.** 1999. Targeted gene mutations define the roles of insulin and IGF-I receptors in mouse embryonic development. J. Pediatr. Endocrinol. Metab. **12:**475–485.
2. **Allen, J. D., and A. Berns.** 1996. Complementation tagging of cooperating oncogenes in knockout mice. Semin. Cancer Biol. **7:**299–306.
3. **Allen, J. D., E. Verhoeven, J. Domen, M. van der Valk, and A. Berns.** 1997. Pim-2 transgene induces lymphoid tumors, exhibiting potent synergy with c-myc. Oncogene **15:**1133–1141.
4. **Baytel, D., S. Shalom, I. Madgar, R. Weissenberg, and J. Don.** 1998. The human Pim-2 proto-oncogene and its testicular expression. Biochim. Biophys. Acta **1442:**274–285. (Erratum, **1444:**312–313, 1999.)
5. **Berns, A., H. Mikkers, P. Krimpenfort, J. Allen, B. Scheijen, and J. Jonkers.** 1999. Identification and characterization of collaborating oncogenes in compound mutant mice. Cancer Res. **59:**1773s–1777s.
6. **Borg, K. E., M. Zhang, D. Hegge, R. L. Stephen, D. J. Buckley, N. S. Magnuson, and A. R. Buckley.** 1999. Prolactin regulation of pim-1 expres-

sion: positive and negative promoter elements. Endocrinology **140:**5659–5668.
7. **Cuypers, H. T., G. Selten, W. Quint, M. Zijlstra, E. R. Maandag, W. Boelens, P. van Wezenbeek, C. Melief, and A. Berns.** 1984. Murine leukemia virus-induced T-cell lymphomagenesis: integration of proviruses in a distinct chromosomal region. Cell **37:**141–150.
8. **Dautry, F., D. Weil, J. Yu, and A. Dautry-Varsat.** 1988. Regulation of pim and myb mRNA accumulation by interleukin 2 and interleukin 3 in murine hematopoietic cell lines. J. Biol. Chem. **263:**17615–17620.
9. **Domen, J., N. M. van der Lugt, D. Acton, P. W. Laird, K. Linders, and A. Berns.** 1993. Pim-1 levels determine the size of early B lymphoid compartments in bone marrow. J. Exp. Med. **178:**1665–1673.
10. **Domen, J., N. M. van der Lugt, P. W. Laird, C. J. Saris, A. R. Clarke, M. L. Hooper, and A. Berns.** 1993. Impaired interleukin-3 response in Pim-1-deficient bone marrow-derived mast cells. Blood **82:**1445–1452.
11. **Eichmann, A., L. Yuan, C. Breant, K. Alitalo, and P. J. Koskinen.** 2000. Developmental expression of pim kinases suggests functions also outside of the hematopoietic system. Oncogene **19:**1215–1224.
12. **Feldman, J. D., L. Vician, M. Crispino, G. Tocco, V. L. Marcheselli, N. G. Bazan, M. Baudry, and H. R. Herschman.** 1998. KID-1, a protein kinase induced by depolarization in brain. J. Biol. Chem. **273:**16535–16543.
13. **Fox, C. J., P. S. Hammerman, R. M. Cinalli, S. R. Master, L. A. Chodosh, and C. B. Thompson.** 2003. The serine/threonine kinase Pim-2 is a transcriptionally regulated apoptotic inhibitor. Genes Dev. **17:**1841–1854.
14. **Gibson, L. F., D. Piktel, and K. S. Landreth.** 1993. Insulin-like growth factor-1 potentiates expansion of interleukin-7-dependent pro-B cells. Blood **82:**3005–3011.
15. **Hardy, R. R., and K. Hayakawa.** 2001. B cell development pathways. Annu. Rev. Immunol. **19:**595–621.
16. **Hess, J., A. Werner, T. Wirth, F. Melchers, H. M. Jack, and T. H. Winkler.** 2001. Induction of pre-B cell proliferation after de novo synthesis of the pre-B cell receptor. Proc. Natl. Acad. Sci. USA **98:**1745–1750.
17. **Ihle, J. N., W. Thierfelder, S. Teglund, D. Stravapodis, D. Wang, J. Feng, and E. Parganas.** 1998. Signaling by the cytokine receptor superfamily. Ann. N. Y. Acad. Sci. **865:**1–9.
18. **Jacobs, H., P. Krimpenfort, M. Haks, J. Allen, B. Blom, C. Demolliere, A. Kruisbeek, H. Spits, and A. Berns.** 1999. PIM1 reconstitutes thymus cellularity in interleukin 7- and common gamma chain-mutant mice and permits thymocyte maturation in Rag- but not CD3γ-deficient mice. J. Exp. Med. **190:**1059–1068.
19. **Johnson, E. W., L. A. Jones, and R. W. Kozak.** 1992. Expression and function of insulin-like growth factor receptors on anti-CD3-activated human T lymphocytes. J. Immunol. **148:**63–71.
20. **Laird, P. W., N. M. van der Lugt, A. Clarke, J. Domen, K. Linders, J. McWhir, A. Berns, and M. Hooper.** 1993. In vivo analysis of Pim-1 deficiency. Nucleic Acids Res. **21:**4750–4755.
21. **Lantz, O., I. Grandjean, P. Matzinger, and J. P. Di Santo.** 2000. Gamma chain required for naive $CD4^+$ T-cell survival but not for antigen proliferation. Nat. Immunol. **1:**54–58.
22. **Lilly, M., T. Le, P. Holland, and S. L. Hendrickson.** 1992. Sustained expression of the pim-1 kinase is specifically induced in myeloid cells by cytokines whose receptors are structurally related. Oncogene **7:**727–732.
23. **Lilly, M., J. Sandholm, J. J. Cooper, P. J. Koskinen, and A. Kraft.** 1999. The PIM-1 serine kinase prolongs survival and inhibits apoptosis-related mitochondrial dysfunction in part through a bcl-2-dependent pathway. Oncogene **18:**4022–4031.
24. **Matikainen, S., T. Sareneva, T. Ronni, A. Lehtonen, P. J. Koskinen, and I. Julkunen.** 1999. Interferon-alpha activates multiple STAT proteins and upregulates proliferation-associated IL-2Rα, c-myc, and pim-1 genes in human T cells. Blood **93:**1980–1991.
25. **Mikkers, H., J. Allen, P. Knipscheer, L. Romeyn, A. Hart, E. Vink, and A. Berns.** 2002. High-throughput retroviral tagging to identify components of specific signaling pathways in cancer. Nat. Genet. **32:**153–159.
26. **Miura, O., Y. Miura, N. Nakamura, F. W. Quelle, B. A. Witthuhn, J. N. Ihle, and N. Aoki.** 1994. Induction of tyrosine phosphorylation of Vav and expression of Pim-1 correlates with Jak2-mediated growth signaling from the erythropoietin receptor. Blood **84:**4135–4141.
27. **Moriggl, R., D. J. Topham, S. Teglund, V. Sexl, C. McKay, D. Wang, A. Hoffmeyer, J. van Deursen, M. Y. Sangster, K. D. Bunting, G. C. Grosveld, and J. N. Ihle.** 1999. Stat5 is required for IL-2-induced cell cycle progression of peripheral T cells. Immunity **10:**249–259.
28. **Moroy, T., A. Grzeschiczek, S. Petzold, and K. U. Hartmann.** 1993. Expression of a Pim-1 transgene accelerates lymphoproliferation and inhibits apoptosis in lpr/lpr mice. Proc. Natl. Acad. Sci. USA **90:**10734–10738.
29. **Mountford, P., B. Zevnik, A. Duwel, J. Nichols, M. Li, C. Dani, M. Robertson, I. Chambers, and A. Smith.** 1994. Dicistronic targeting constructs: reporters and modifiers of mammalian gene expression. Proc. Natl. Acad. Sci. USA **91:**4303–4307.
30. **Nieborowska-Skorska, M., G. Hoser, P. Kossev, M. A. Wasik, and T. Skorski.** 2002. Complementary functions of the antiapoptotic protein A1 and serine/threonine kinase pim-1 in the BCR/ABL-mediated leukemogenesis. Blood **99:**4531–4539.
31. **Nosaka, T., T. Kawashima, K. Misawa, K. Ikuta, A. L. Mui, and T. Kitamura.** 1999. STAT5 as a molecular regulator of proliferation, differentiation and apoptosis in hematopoietic cells. EMBO J. **18:**4754–4765.
32. **Palaty, C. K., G. Kalmar, G. Tai, S. Oh, L. Amankawa, M. Affolter, R. Aebersold, and S. L. Pelech.** 1997. Identification of the autophosphorylation sites of the *Xenopus laevis* Pim-1 proto-oncogene-encoded protein kinase. J. Biol. Chem. **272:**10514–10521.
33. **Pircher, T. J., S. Zhao, J. N. Geiger, B. Joneja, and D. M. Wojchowski.** 2000. Pim-1 kinase protects hematopoietic FDC cells from genotoxin-induced death. Oncogene **19:**3684–3692.
34. **Saris, C. J., J. Domen, and A. Berns.** 1991. The pim-1 oncogene encodes two related protein-serine/threonine kinases by alternative initiation at AUG and CUG. EMBO J. **10:**655–664.
35. **Selten, G., H. T. Cuypers, and A. Berns.** 1985. Proviral activation of the putative oncogene Pim-1 in MuLV induced T-cell lymphomas. EMBO J. **4:**1793–1798.
36. **Shirogane, T., T. Fukada, J. M. Muller, D. T. Shima, M. Hibi, and T. Hirano.** 1999. Synergistic roles for Pim-1 and c-Myc in STAT3-mediated cell cycle progression and antiapoptosis. Immunity **11:**709–719.
37. **Sicinski, P., J. L. Donaher, S. B. Parker, T. Li, A. Fazeli, H. Gardner, S. Z. Haslam, R. T. Bronson, S. J. Elledge, and R. A. Weinberg.** 1995. Cyclin D1 provides a link between development and oncogenesis in the retina and breast. Cell **82:**621–630.
38. **Teglund, S., C. McKay, E. Schuetz, J. M. van Deursen, D. Stravopodis, D. Wang, M. Brown, S. Bodner, G. Grosveld, and J. N. Ihle.** 1998. Stat5a and Stat5b proteins have essential and nonessential, or redundant, roles in cytokine responses. Cell **93:**841–850.
39. **Telerman, A., R. Amson, R. Zakut-Houri, and D. Givol.** 1988. Identification of the human pim-1 gene product as a 33-kilodalton cytoplasmic protein with tyrosine kinase activity. Mol. Cell. Biol. **8:**1498–1503.
40. **Temple, R., E. Allen, J. Fordham, S. Phipps, H. C. Schneider, K. Lindauer, I. Hayes, J. Lockey, K. Pollock, and R. Jupp.** 2001. Microarray analysis of eosinophils reveals a number of candidate survival and apoptosis genes. Am. J. Respir. Cell Mol. Biol. **25:**425–433.
41. **te Riele, H., E. R. Maandag, A. Clarke, M. Hooper, and A. Berns.** 1990. Consecutive inactivation of both alleles of the pim-1 proto-oncogene by homologous recombination in embryonic stem cells. Nature **348:**649–651.
42. **Tough, D. F., and J. Sprent.** 1995. Lifespan of lymphocytes. Immunol. Res. **14:**1–12.
43. **Trumpp, A., Y. Refaeli, T. Oskarsson, S. Gasser, M. Murphy, G. R. Martin, and J. M. Bishop.** 2001. c-Myc regulates mammalian body size by controlling cell number but not cell size. Nature **414:**768–773.
44. **van der Lugt, N. M., J. Domen, E. Verhoeven, K. Linders, H. van der Gulden, J. Allen, and A. Berns.** 1995. Proviral tagging in E mu-myc transgenic mice lacking the Pim-1 proto-oncogene leads to compensatory activation of Pim-2. EMBO J. **14:**2536–2544.
45. **Verbeek, S., M. van Lohuizen, M. van der Valk, J. Domen, G. Kraal, and A. Berns.** 1991. Mice bearing the Eμ-*myc* and Eμ-*pim*-1 transgenes develop pre-B-cell leukemia prenatally. Mol. Cell. Biol. **11:**1176–1179.
46. **Wang, Z., N. Bhattacharya, M. K. Meyer, H. Seimiya, T. Tsuruo, J. A. Tonani, and N. S. Magnuson.** 2001. Pim-1 negatively regulates the activity of PTP-U2S phosphatase and influences terminal differentiation and apoptosis of monoblastoid leukemia cells. Arch. Biochem. Biophys. **390:**9–18.
47. **Wingett, D., A. Long, D. Kelleher, and N. S. Magnuson.** 1996. pim-1 proto-oncogene expression in anti-CD3-mediated T cell activation is associated with protein kinase C activation and is independent of Raf-1. J. Immunol. **156:**549–557.
48. **Yip-Schneider, M. T., M. Horie, and H. E. Broxmeyer.** 1995. Transcriptional induction of pim-1 protein kinase gene expression by interferon gamma and posttranscriptional effects on costimulation with steel factor. Blood **85:**3494–3502.